[1] Jinjin Chen
[1] Quan Zhou
[1] Yueming Cai
[2] Bin Liu*

Multiple-Points Dam Deformation Modeling and Prediction Based on Extreme Learning Machine

***Abstract:* -** The multiple-points dam deformation model establishes vital connections among monitoring points on the dam, which are crucial for assessing the overall behavior of the dam. This study examines the statistical process of the multiple-point dam deformation model and introduces three methods: extreme learning machine, backpropagation neural networks, and stepwise regression for modeling multiple-point dam deformation. In the case study of Wuqiangxi Dam, the performance of the three multiple point models is analyzed and evaluated. Multiple-points dam deformation models are shown to be effective in modeling and predicting the displacements of all monitoring points on one tension wire at the same time, though the performance of the models would present different results at different monitoring points. All three models yielded satisfactory results, with average fitting residual RMS values of 1.12 mm, 0.91 mm, and 1.15 mm, and average prediction residual RMS values of 1.68 mm, 1.76 mm, and 1.61 mm, respectively. The fitting and prediction results indicate the feasibility of multiple-points dam deformation model. In comparison to the other two methods, the extreme learning machine-based multiple-point model, serving as a single hidden-layer feedforward neural network, demonstrates the advantages of simplicity, flexibility, and efficiency.

Keywords: multiple-points model, dam behavior, extreme learning machine, back-propagation neural networks, stepwise regression

1 INTRODUCTION

The in-depth analysis and modeling of dam deformation data serve as a crucial basis for evaluating its safety and guiding engineering decisions [1]. This deformation process is significantly influenced by environmental conditions such as temperature fluctuations, water level changes, and pore pressure. By establishing an accurate deformation model, we can predict how the dam responds to these environmental changes, thereby better explaining and predicting the overall behavior of the dam.

Statistical and deterministic models are the main approaches to evaluate the response of the dam[2]. In the case of deterministic models, the response of the dam's structure is approximated by applying physical principles through the finite element method. This quantitative approach is intricate and computationally challenging, often hindered by limited understanding of the stress-strain characteristics of dam and foundation materials [3]. Consequently, statistical models have gained wider acceptance and application in modeling dam deformations. They offer advantages over deterministic models, including simpler formulations, faster execution, and the capability to capture any correlation between effective and response variables [2]. Among statistical methods, multiple linear regression models prevail in dam deformation modeling [4, 5], utilizing least squares estimation of coefficients to delineate the relationship between deformation displacements and contributing factors. Taking into account the multicollinearity that exists between the independent variables, some improved regression methods are proposed in the modeling, such as stepwise regression (SMR)[6], partial least squares regression [7], principal component regression [8] and independent component regression [9]. In these improved regression models, the variables considered insignificant are ignored, which can cause the loss of important information in some cases [10].

With the continuous evolution of artificial intelligence technology, various neural network algorithms have been innovatively applied to the field of dam deformation modeling, becoming a research hotspot [3,4,10-20]. Among them, the Extreme Learning Machine (ELM), first proposed by scholars such as Huang [21,22], demonstrates significant advantages over traditional feedforward network learning algorithms: it not only possesses stronger generalization capabilities but also achieves a qualitative leap in learning speed [23]. As one of the fastest and relatively efficient machine learning approaches, ELM has been a focal point in machine learning research. Research on ELM primarily encompasses algorithm refinement and application studies. An example of an innovative approach is the data classification method introduced by Liu et al., which utilizes a combination of Particle Swarm

[1]* Hunan institute of metrology and test, Changsha 410014, Hunan, China.
[2]School of Traffic and Transportation, Changsha University of Science and Technology, Changsha, 410114, China. Email:csust_bin@163.com

Optimization and Kernel Extreme Learning Machines [24]. Meanwhile, Bacanin et al. have proposed a multi-swarm hybrid optimization technique aimed at identifying optimal or near-optimal weights and biases within hidden layers for specific tasks [25]. Additionally, ELM has found extensive applications across various fields of study such as medical benchmark dataset classification [26], Internet of Things security [27], the diagnosis of anemiat[28], and online dynamic security assessment of power systems[29].

Traditional dam deformation models have primarily relied on single monitoring points, limiting their effectiveness for comprehensive dam deformation analysis and health diagnosis. Consequently, recent studies have focused on concurrently modeling dam deformations across multiple monitoring points and the entire dam structure by employing refined mathematical techniques [30-35]. While various machine learning methods have been extensively used in dam deformation modeling [3, 4, 10-20], there has been limited focus on modeling for multiple monitoring points. For instance, Kang et al. proposed an ELM-based health monitoring model for dam displacement prediction, which is known for its simplicity in operation, fast speed, and superior prediction performance [10]. Based on their work, ELM was applied in the modeling of multiple-points horizontal dam deformation model in encompassing the positional data of dam monitoring points as part of the input variables. At the same time, two other methods based on BP and SMR were also introduced in the mutiple-points dam deformation modeling and compared with the results of ELM derived model. All the three multiple-point models were proved to be effective in modeling and predicting the displacements of all the monitoring points on one tension wire concurrently. Additionally, the ELM-based multi-point model exhibits enhanced stability and superior generalization.

The organization of this paper comprises the following sections: Section 2 delves into the ELM algorithm and outlines the multi-point dam deformation model. Section 3 features a case analysis of the multi-point dam deformation model applied to Wuqaingxi Dam, utilizing ELM, the backpropagation (BP) neural network, and stepwise regression. This section also engages in a comparative evaluation and discussion of the performance exhibited by these three methodologies. Lastly, Section 4 concludes the paper by summarizing the key findings and outlining directions for future research endeavors.

2 MODELING METHODS

2.1 Extreme learning machine

The extreme learning machine is a feedforward neural network method for a single hidden layer, for the given N arbitrary distinct training (x_i, t_i), in which $x_i = [x_{i1}, x_{i2}, \cdots, x_{in}]^T \in R^n$, and $t_i = [t_{i1}, t_{i2}, \cdots, t_{im}]^T \in R^m$, the activation function of single hidden layer feedforward neural network with $\tilde{N}$ hidden nodes is expressed as:

$$\sum_{i=1}^{\tilde{N}} \beta_i g(w_i \cdot x_j + b_i) = t_j, \quad j = 1,2,\cdots,N.$$
$$w_i = [w_{i1}, w_{i2}, \cdots, w_{in}]^T; \tag{1}$$
$$\beta_i = [\beta_{i1}, \beta_{i2}, \cdots, \beta_{im}]^T$$

where w_i is the weight of the input layer and the ith hidden layer, β_i is the weight of the ith hidden layer and the output layer, b_i Is the threshold value of the ith hidden layer nodes, $g(x)$ is the activation function.

If the activation function is regarded as a matrix abbreviated by H, then Formula (1) can be simplified as follows:

$$H\beta = T \tag{2}$$

where H is the output of the hidden layer node, β is the output weight, and T is the expected output. Their expressions are as follows:

$$(w_1, \cdots, w_{\tilde{N}},\ b_1, \cdots, b_{\tilde{N}},\ x_1, \cdots, x_{\tilde{N}}) = \begin{bmatrix} g(w_1 \cdot x_1 + b_1) & \cdots & g(w_{\tilde{N}} \cdot x_1 + b_{\tilde{N}}) \\ \vdots & \cdots & \vdots \\ g(w_1 \cdot x_N + b_1) & \cdots & g(w_{\tilde{N}} \cdot x_N + b_{\tilde{N}}) \end{bmatrix}_{N\times\tilde{N}} \tag{3}$$

$$\beta = \begin{bmatrix} \beta_1^T \\ \vdots \\ \beta_{\tilde{N}}^T \end{bmatrix}_{\tilde{N}\times m}, \qquad T = \begin{bmatrix} t_1^T \\ \vdots \\ t_{\tilde{N}}^T \end{bmatrix}_{N\times m} \tag{4}$$

where the matrix H is the output matrix of the hidden layer of the neural network.

For a linear system $Ax = y$, if Formula (5) is satisfied, then $\hat{x}$ is the least square solution of the linear system:

$$\|A\hat{x} - y\| = \min_x \|Ax - y\| \tag{5}$$

In the context of Extreme Learning Machines (ELM), when the activation function is infinitely differentiable, the determination of the input weights and hidden node thresholds of the single-hidden layer feedforward neural network uniquely specifies the output matrix of the hidden layer. Consequently, training this neural network can be reduced to solving a linear system. This process is equivalent to finding the least squares solution, denoted as $\hat{\beta}$, for the linear system in Equation (1).

$$\left\|H\left(w_1, \cdots, w_{\tilde{N}},\ b_1, \cdots, b_{\tilde{N}}\right)\hat{\beta} - T\right\| = \min_\beta \left\|H\left(w_1, \cdots, w_{\tilde{N}},\ b_1, \cdots, b_{\tilde{N}}\right)\beta - T\right\| \tag{6}$$

According to the definition of the generalized inverse matrix, the minimum norm of the least squares solution of the linear system h $H\beta = T$ is:

$$\hat{\beta} = H^{\dagger}T \tag{7}$$

where $H^{\dagger}$ is the Moore Penrose generalized inverse of matrix H, and it can be proved that the norm of the solution $\hat{\beta}$ is the smallest and unique.

2.2 Multiple Points Dam Deformation Modeling

Statistical dam deformation model

The deformation phenomenon of dams can be simulated and predicted by constructing statistical models that incorporate external variables such as hydrostatic pressure, ambient temperature, and time (e.g., HST or HTT models) [36, 37]. Among these factors, hydrostatic pressure (H), ambient temperature (T), and time (θ) are considered the three key factors that play a dominant role in dam deformation. Thus, the dam deformation model can be expressed as [1, 2, 4, 9]:

$$Y = f(H, T, \theta) = Y_H + Y_T + Y_\theta \tag{8}$$

where Y represents the dam deformation, and Y_H, Y_T and Y_θ are the deformations due to hydrostatic load, changes in temperature, and time.

The deformations Y_H can be described as a polynomial function of the water level as:

$$Y_H = a_1 H + a_2 H^2 + a_3 H^3 \tag{9}$$

where H is the water level difference between the upstream and the downstream, and $a_i\ (i = 1,2,3)$ are the unknown coefficients of the hydrostatic factors.

Thermal expansion of the dam body due to temperature changes is another main factor of dam deformation. Taking into account the deferred effects of the ambient temperature to the dam, the following formula is used to model the temperature related deformations:

$$Y_T = b_1 T_1 + b_2 T_2 + b_3 T_3 + b_4 T_4 \tag{10}$$

where $b_i\ (i = 1,2,3,4)$ are the unknown coefficients, and $T_i\ (i = 1,2,3,4)$ represents the average temperatures of the observation date, 2~7 days, 8~30 days, and 31~60 days before the observation date, respectively.

The third notable characteristic of dam deformation is the aging component, which represents the irreversible displacement changes that occur over time. This deformation phenomenon can be described and predicted by constructing a model using specific mathematical equations.

$$Y_\theta = c_1\theta + c_2\ln\theta \tag{11}$$

where the c_i $(i = 1,2)$ are the unknown coefficients, and θ is a variable defined as $\theta = (t - t_0)/365$, where t is the observation date and t_0 is the initial date in the modeling.

Therefore, in the MLR-based and other statistical dam deformation models, the following detailed formula can be applied:

$$Y = a_0 + \sum_{i=1}^{3} a_i H^i + \sum_{j=1}^{4} b_j T_j + c_1\theta + c_2\ln\theta \tag{12}$$

where a_0 is the constant term.

Inputs of the Multiple Point Dam Deformation Model

In the model of multiple-point dam deformation model, the location parameters (x, y, z) are introduced in the models. For the dam monitoring points in one tension wire on the dam, namely, one-dimensional multi-point model, one positional parameter (x) of the monitoring points is introduced in the Formula (8), and the model can be expressed as follows:

$$Y = f(H, T, \theta, x) = Y_{H,x} + Y_{T,x} + Y_{\theta,x} \tag{13}$$

where the $Y_{H,x}$, $Y_{T,x}$ and $Y_{\theta,x}$ are the deformations due to the hydrostatic load, temperature changes and time combined with positional parameter.

Taking into account the complex influence of the positional parameter x on the deformation of the monitoring point, the different power of x are introduced in the multiple-points dam and arranged and combined with other variables. The detailed selections of parameters are shown in Table 1. Totally 15 hydrostatic factors, 16 temperature factors, and 4 time factors are selected as the inputs in the multiple-point dam deformation model.

Table 1. Selection of the input variables in the multiple-point dam deformation model

	Hydrostatic factors	Temperature factors	Time factors
Input variables	Hx^{-1}, H, Hx, Hx^2, H^2x^{-1}, H^2, , H^2x, H^2x^2, H^3x^{-1}, H^3, H^3x, H^3x^2, x, x^2, x^3	T_j, T_jx, T_jx^2, T_jx^3	θ, $\ln\theta$, $x\theta$, $x\ln\theta$

*The parameters H, T_j and θ are same with those in Formula (12)

3 CASE STUDY OF THE WUQAINGXI DAM

3.1 Description of Wuqiangxi Dam Monitoring Data Sets

The Wuqiangxi Dam, a magnificent project located in Hunan and completed in 1994, boasts a length of 724.4 meters and a height of 85.8 meters. Its massive reservoir has a capacity of up to 429 million cubic meters. To ensure the safety and stability of the dam, an advanced automatic monitoring system has been installed, which comprehensively covers various aspects such as tension alignment, inverted pendulum observation, water level monitoring, and seepage conditions. In Figure 1, we can clearly see the upstream view of the dam and the precise monitoring of horizontal displacement through tension wires (ex1 and ex2). Figure 2 shows the distribution of the two alignments of the tension wires and inverted plumbs.

(a) (b)

Fig.1. (a) Wuqiangxi Dam and (b) tension wire measurements.

In the case study, daily monitoring data of horizontal displacements from April 2004 to February 2010 on the tension wire ex2 are used. As depicted in Figure 3, the modeling process incorporated the daily variations in water levels between the upstream and downstream regions, as well as the corresponding air temperature data. The data sets for the next half year, from March to August 2010, were reserved as test data to assess the predictive capability of the deformation models. Due to poor quality, monitoring points ex2_22 and ex2_23 were excluded from the case study, resulting in the selection of 21 monitoring points for the modeling. The detection of outliers in the monitoring datasets was performed using triple standard deviations, and a space-time Kalman filtering method was applied to filter noise and interpolate missing data [31]. Utilizing the one-dimensional positional coordinates of monitored points, along with temperature and water level data, 39 input variables were derived for the multiple-points model as outlined in Table 1. Normalization was conducted on each variable to mitigate the impact of numerical values.

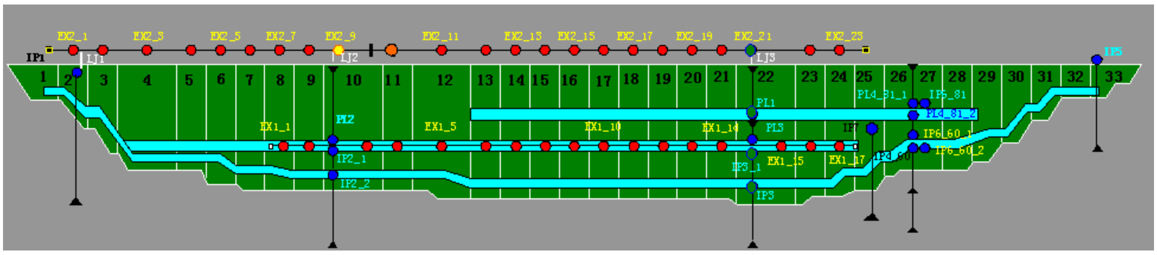

Fig. 2. Distribution of the two alignments of the tension wires and inverted plumbs.

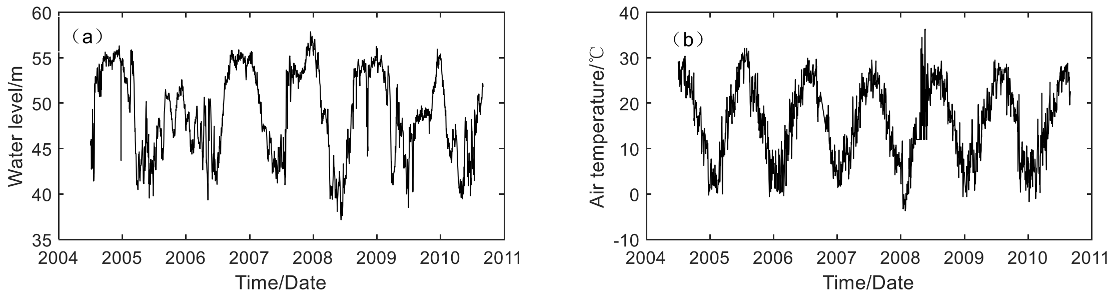

Fig. 3. The monitored daily (a) water level and (b) air temperature data.

3.2 Modeling and the results

In the case study, we developed a multi-point deformation prediction model that integrates ELM, BP neural network, and SMR technology. Specifically, the ELM model employs an S-shaped function as the activation mechanism, and the number of hidden layer nodes was determined through repeated experiments and adjustments to be 100, ensuring optimal model performance. The 39 parameters in Tab.1 were seen as inputs and the monitored displacements of the 21 points were seen as output in the modeling.

Drawing upon the research in [10], this paper employs a BP neural network, initializing weights and biases through the Nguyen Widrow method. The number of hidden layer nodes is determined to be 3 through trial and error, resulting in a neural network structure of 10-21-1. During training, 1000 epochs are set, with a mean squared error (MSE) training target of 0.001. For the hidden layer, the hyperbolic tangent sigmoid function is chosen as the transfer function, while the output layer employs a linear transfer function.

To be noticed, the problem of 'overfitting' is existed in the ELM and BP neural network modeling process, which affects the performance of the prediction results. In the actual operation, cross-validation and early stopping were adopted to ensure better training and testing performance [38]. Considering the different results achieved in each separate run in ELM and BP neural network model due to the initial random weights, ten continuous runs were conducted for the ELM and BP network, and the mean values of the training and prediction results were achieved and used to evaluate the performance of the model. The fitting and prediction results are shown in Figure 4 and 5.

For comparisons, traditional SMR was also adopted in the modeling of multiple points dam deformation. The constant term and the same 35 inputs as in Table 1 were selected as independent variables in the regression model. The fitting and prediction result for each monitoring point is presented in Figure 6.

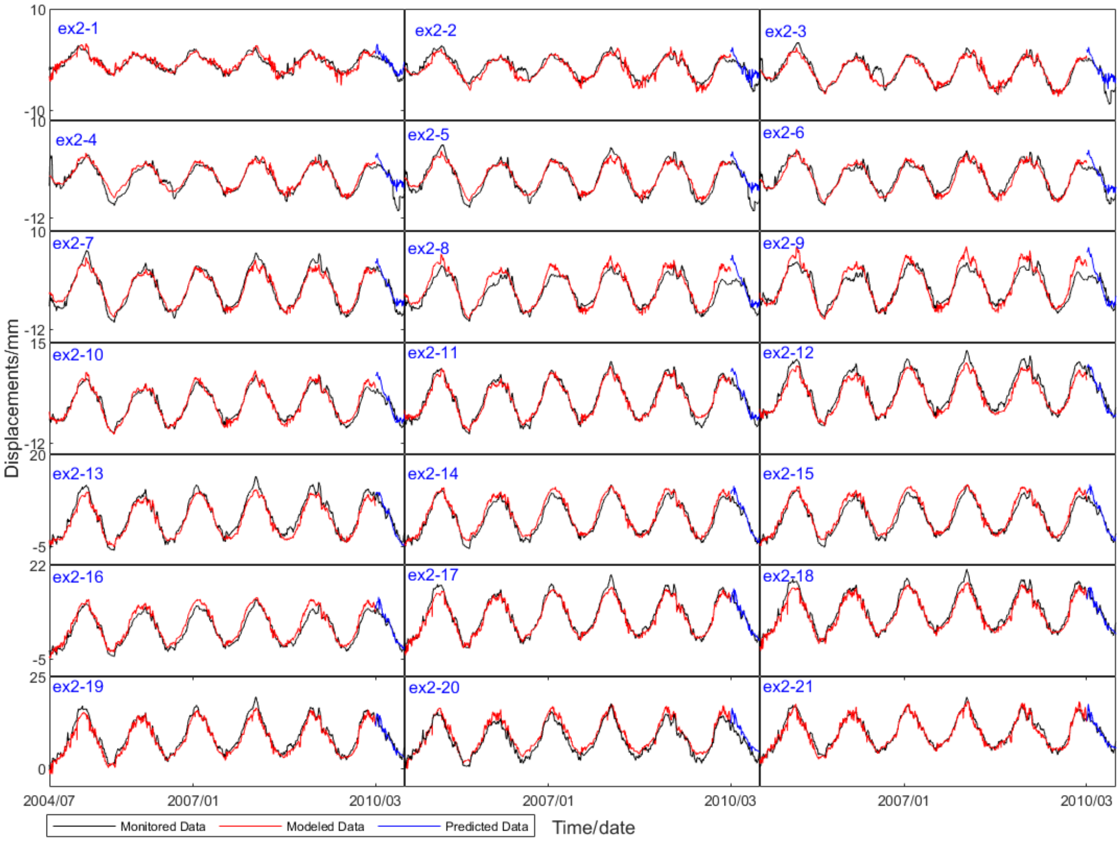

Fig. 4. Performance of fitting and prediction for the ELM-based multiple-point dam deformation model

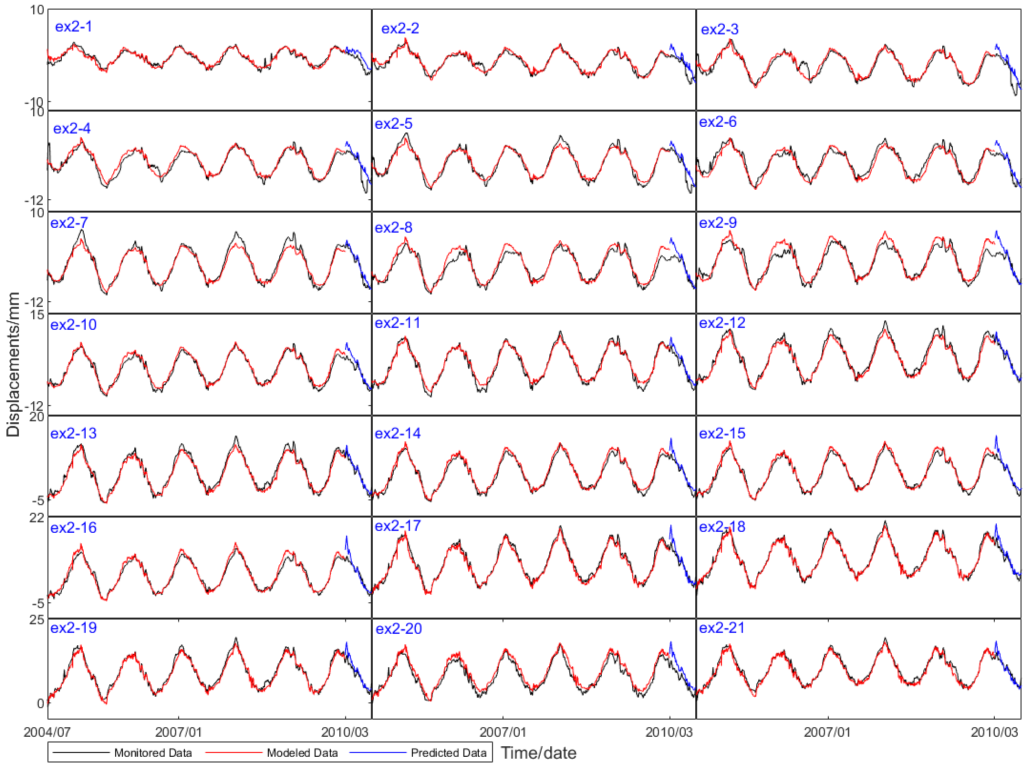

Fig. 5. Performance of fitting and prediction for the BP-based multiple-point dam deformation model

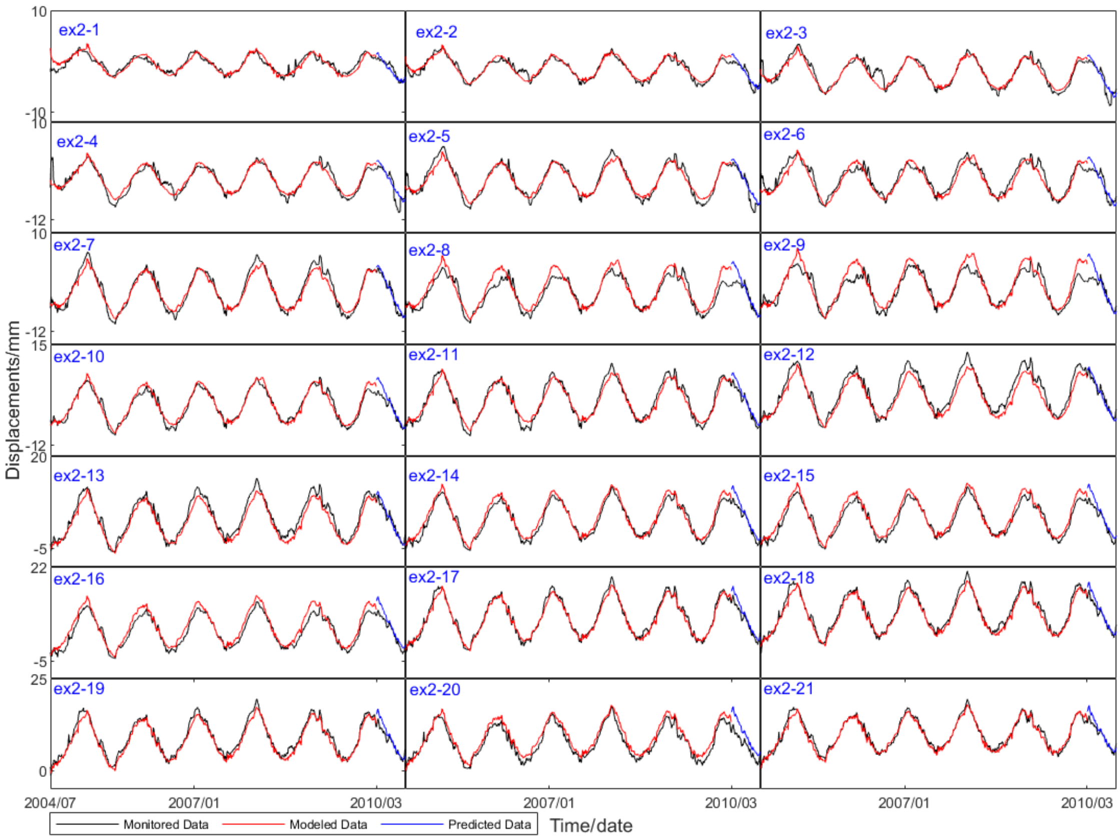

Fig. 6. Performance of fitting and prediction for the SMR-based multiple-point dam deformation model

3.4 Comparisons and Discussion

As evident from Figures 4, 5, and 6, the modeled outcomes demonstrate a satisfactory alignment with the monitored data pertaining to tension wire exx2, encompassing predictions across all monitoring points. While the accuracy of fitting and prediction is average for certain points, the root mean square (RMS) values of residuals were computed to provide a comprehensive assessment of the varying performance of multiple-point models at different points. The results of this analysis are presented in Table 2.

Table 2 The RMS values of the fitting and prediction results of the different models for each monitoring point (mm).

Monitoring Points	**ELM**		**BP**		**SMR**	
	Fitting	**Prediction**	**Fitting**	**Prediction**	**Fitting**	**Prediction**
ex2_1	0.72	1.28	0.48	1.13	0.67	0.72
ex2_2	0.75	1.82	0.56	1.57	0.62	0.92
ex2_3	0.76	2.13	0.79	2.09	0.84	1.29
ex2_4	0.96	2.42	0.92	2.45	0.96	1.71
ex2_5	0.92	2.25	0.84	2.23	0.97	1.54
ex2_6	1.03	1.85	1.02	1.75	1.22	1.56
ex2_7	1.09	1.29	1.06	1.08	1.04	0.93
ex2_8	1.41	2.01	1.16	1.73	1.54	2.08
ex2_9	1.46	1.95	1.31	2.01	1.64	2.46
ex2_10	0.92	1.54	0.83	1.75	0.98	1.94
ex2_11	1.10	1.45	0.92	2.02	1.16	1.42
ex2_12	1.50	0.99	1.08	1.83	1.76	1.05
ex2_13	1.31	0.85	1.02	1.50	1.50	1.09
ex2_14	1.19	1.70	0.86	1.39	1.17	1.83
ex2_15	1.27	1.87	0.82	1.34	1.29	2.02
ex2_16	1.46	1.79	0.97	1.49	1.59	2.01
ex2_17	0.96	1.41	0.82	2.52	0.82	1.60
ex2_18	1.17	1.25	0.72	2.27	1.04	1.44
ex2_19	1.10	1.32	0.83	1.60	1.04	1.63
ex2_20	1.40	2.80	1.32	2.27	1.38	3.24
ex2_21	0.99	1.20	0.86	0.89	0.83	1.36
Average	1.12	1.68	0.91	1.76	1.15	1.61

Generally speaking, considering that the multiple-points model is aimed at modeling the deformations for all the monitoring points on one tension wire at the same time, the fitting and prediction results of all the three multiple points were with satisfying results. The RMS values of the fitting results are around 1mm and the prediction results are around 1.7mm. In the BP modeling, early stopping was adopted, but the 'overfitting' problem still occurred some times and affected the performance of the BP model, getting the best fitting result but the worst prediction result, with RMS values of 0.91mm and 1.76mm, respectively. To evaluate the performance of the three multiple-points models, additional metrics including the Mean Absolute Error (MAE), Mean Absolute Percentage Error (MAPE), and the Coefficient of Determination (R^2) were calculated. The results are shown in Table 3. From the perspective of MAE values, the modeling effects of the three models are similar to those obtained from RMS, with BP is with the best fitting effect and the worst prediction effect. The BP model performed the worst in MAPE results, while SMR obtained the best results. The R^2 values of the three models are very similar, with fitting and prediction results around 0.96 and 0.90, respectively Compared with the BP model, ELM was with better generalization and more stable results. In addition, the time cost of the ELM and SMR models is much less than that of the BP model.

Table 3 The MAE、MAPE and R^2 of the three multiple-points dam deformation models

Methods	**MAE/mm**		**MAPE**		$\mathbf{R^2}$	
	Fitting	**Prediction**	**Fitting**	**Prediction**	**Fitting**	**Prediction**
ELM	0.93	1.35	2.95	2.03	0.96	0.90
BP	0.85	1.54	3.01	2.67	0.97	0.88
SMR	0.93	1.28	1.95	1.69	0.96	0.91

However, the performance of the multiple-points models on different monitoring points is with obvious differences, which are thought to be caused by the degree of correlation of the deformations. For example, the RMS values of points ex2_8, ex2_9, and ex2_20 are relative larger than those of the mean value for all the three models, indicating poorer model performance at these points. The monitored displacements on these points may exhibit more localized deformations, and the multiple-point models are insensitive to these localized deformations.

Table 4 The regression coefficients of the SMR multiple-point model

Factors	**Coefficients**	**Factors**	**Coefficients**	**Factors**	**Coefficients**
Hx^{-1}	-3.45	x	181.66	T_2x^2	0.00
H	38.11	x^2	-132.57	T_3x^2	-8.87
Hx	-592.68	x^3	-12.31	T_4x^2	19.13
Hx^2	471.48	T_1,	-0.18	T_1x^3	3.36
H^2x^{-1}	6.53	T_2	-0.26	T_2x^3	0.00
H^2	-81.92	T_3	-0.64	T_3x^3	5.59
H^2x	640.25	T_4	-0.50	T_4x^3	-8.35
H^2x^2	-492.23	T_1x	2.25	θ	0.45
H^3x^{-1}	-3.16	T_2x	-1.02	$\ln\theta$	-0.96
H^3	44.10	T_3x	2.46	$x\theta$	-0.37
H^3x,	-233.83	T_4x	-11.37	$x\ln\theta$	3.01
H^3x^2	173.14	T_1x^2	-5.59	Const	1.63

*The parameters H, T_j and θ are same with those in Formula (12);

*Const represents the constant term in the regression model.

The regression coefficients obtained from the SMR model are presented in Table 4. The regression model assumes independence among the variables, enabling the identification of each factor's individual contribution to the structural response through their respective coefficients. It is noticed that the coefficients in Table 3 are unreasonable relative to the displacement range since all inputs had been normalized. Although we replaced multiple linear regression with stepwise regression in the modeling, there existed series of ill-conditioning of the coefficient matrix, whose condition number is as high as 1.60×10^{10}, indicating that the SMR-based multiple-points model may be not reliable.

4 CONCLUSIONS

In the study, three different methods were proposed in modeling and predicting multiple-point dam deformation, and multiple-point models were proved to be effective in modeling and predicting the displacements of all the monitoring points on one tension wire at the same time, and the model was shown to be an effective method for describing the structural behaviors of the entire dam. The displacements of the monitoring points are with spatial correlation and local deformations, thus the performance of the multiple-points dam deformation models present different results at different monitoring points. The established models are more inclined to modeling the entire structure behavior of the dam, and the local behaviors may be ignored to some extent.

Among the three methods, the ELM-based multiple-point model demonstrates greater stability and superior generalization compared to the SMR and BP neural network models. ELM, being a single hidden layer feedforward neural network, exhibited simplicity, flexibility, and efficiency in its practical application during the case study.

The multi-point model presented in this study is specifically applicable to the monitored points along a tension line. In the future, In the future, incorporating two-dimensional or even three-dimensional spatial coordinates of monitored points can lead to the development of a more effectively multi-points dam deformation model. In addition, it is possible to explore the application effects of more machine learning methods in the field of multi-points deformation modeling of dams.

5 DECLARATIONS

Availability of data and materials

Not applicable

Competing interests

The authors declare that they have no competing interests.

AUTHORS' CONTRIBUTIONS

Methodology, J.C. and B.L.; validation, Q.Z. and Y.C.; formal analysis, J.C. and B.L.; investigation, Q.Z. and Y.C.; data curation, J.C.; writing—original draft preparation, J.C.; writing—review and editing, Q.Z., Y.C. and B.L.; supervision, B.L.; funding acquisition, B.L. All authors have read and agreed to the published version of the manuscript

Acknowledgements

Not applicable

REFERENCES

1. Salazar, F., R. Moran, M. A. Toledo and E. Onate. "Data-based models for the prediction of dam behaviour: A review and some methodological considerations." Archives of Computational Methods in Engineering 24 (2017): 1-21. 10.1007/s11831-015-9157-9. <Go to ISI>://WOS:000392193700001.

2. De Sortis, A. and P. Paoliani. "Statistical analysis and structural identification in concrete dam monitoring." Engineering Structures 29 (2007): 110-20. 10.1016/j.engstruct.2006.04.022.

3. Tayfur, G., D. Swiatek, A. Wita and V. P. Singh. "Case study: Finite element method and artificial neural network models for flow through jeziorsko earthfill dam in poland." Journal of Hydraulic Engineering 131 (2005): 431-40.

4. Mata, J. "Interpretation of concrete dam behaviour with artificial neural network and multiple linear regression models." Engineering Structures 33 (2011): 903-10.

5. Yu, Y., X. L. Liu, E. Z. Wang, K. Fang and L. Huang. "Dam safety evaluation based on multiple linear regression and numerical simulation." Rock Mechanics and Rock Engineering 51 (2018): 2451-67. 10.1007/s00603-018-1435-z. <Go to ISI>://WOS:000440580300011.

6. Sharma, M. J. and S. J. Yu. "Stepwise regression data envelopment analysis for variable reduction." Applied Mathematics & Computation 253 (2015): 126-34.

7. Huang, H., B. Chen and C. G. Liu. "Safety monitoring of a super-high dam using optimal kernel partial least squares." Mathematical Problems in Engineering 2015 (2015): 13. 10.1155/2015/571594. <Go to ISI>://WOS:000367944300001.

8. Hong, Y. U., W. U. Zhongru, B. Tengfei and Z. Lan. "Multivariate analysis in dam monitoring data with pca." Science China Technological Sciences 53 (2010): 1088-97.

9. Dai, W. J., B. Liu, X. L. Ding and D. W. Huang. "Modeling dam deformation using independent component regression method." Transactions of Nonferrous Metals Society of China 23 (2013): 2194-200. 10.1016/s1003-6326(13)62717-x. <Go to ISI>://WOS:000325599600047.

10. Kang, F., J. Liu, J. Li and S. Li. "Concrete dam deformation prediction model for health monitoring based on extreme learning machine." Structural Control and Health Monitoring 24 (2017): 10.1002/stc.1997.

11. Hsu, T. Y. and C. H. Loh. "Damage detection accommodating nonlinear environmental effects by nonlinear principal component analysis." Structural Control & Health Monitoring 17 (2010): 338-54.

12. Loh, C. H., C. H. Chen and T. Y. Hsu. "Application of advanced statistical methods for extracting long-term trends in static monitoring data from an arch dam." Structural Health Monitoring 10 (2011): 587-601.

13. Xu, C., D. Yue and C. Deng. "Hybrid ga/simpls as alternative regression model in dam deformation analysis." Engineering Applications of Artificial Intelligence 25 (2012): 468-75. 10.1016/j.engappai.2011.09.020.

14. Xi, G. Y., J. P. Yue, B. X. Zhou and P. Tang. "Application of an artificial immune algorithm on a statistical model of dam displacement." Computers & Mathematics with Applications 62 (2011): 3980-86.

15. Rankovic, V., N. Grujovic, D. Divac and N. Milivojevic. "Development of support vector regression identification model for prediction of dam structural behaviour." Structural Safety 48 (2014): 33-39. 10.1016/j.strusafe.2014.02.004. <Go to ISI>://WOS:000337778400004.

16. Su, H. Z., Z. X. Chen and Z. P. Wen. "Performance improvement method of support vector machine-based model monitoring dam safety." Structural Control & Health Monitoring 23 (2016): 252-66. 10.1002/stc.1767. <Go to ISI>://WOS:000368033700005.

17. Su, H. Z., X. Li, B. B. Yang and Z. P. Wen. "Wavelet support vector machine-based prediction model of dam deformation." Mechanical Systems and Signal Processing 110 (2018): 412-27. 10.1016/j.ymssp.2018.03.022. <Go to ISI>://WOS:000431162900026.

18. Lin, C. N., T. C. Li, S. Y. Chen, X. Q. Liu, C. Lin and S. L. Liang. "Gaussian process regression-based forecasting model of dam deformation." Neural Computing & Applications 31 (2019): 8503-18. 10.1007/s00521-019-04375-7. <Go to ISI>://WOS:000494051000033.

19. Li, F. Q., Z. Z. Y. Wang and G. H. Liu. "Towards an error correction model for dam monitoring data analysis based on cointegration theory." Structural Safety 43 (2013): 12-20. 10.1016/j.strusafe.2013.02.005. <Go to ISI>://WOS:000319493500002.

20. Zou, J., K.-T. T. Bui, Y. Xiao and C. V. Doan. "Dam deformation analysis based on bpnn merging models." Geo-spatial information science 21 (2018): 149-57.

21. Huang, G.-B., Q.-Y. Zhu and C.-K. Siew. "Extreme learning machine: Theory and applications." Neurocomputing 70 (2006): 489-501. 10.1016/j.neucom.2005.12.126.

22. Huang, G. B., H. M. Zhou, X. J. Ding and R. Zhang. "Extreme learning machine for regression and multiclass classification." Ieee Transactions on Systems Man and Cybernetics Part B-Cybernetics 42 (2012): 513-29. 10.1109/tsmcb.2011.2168604. <Go to ISI>://WOS:000302097000018.

23. Huang, G., G. B. Huang, S. J. Song and K. Y. You. "Trends in extreme learning machines: A review." Neural Networks 61 (2015): 32-48. 10.1016/j.neunet.2014.10.001. <Go to ISI>://WOS:000347595400005.

24. Liu, A., D. Zhao and T. Li. "A data classification method based on particle swarm optimisation and kernel function extreme learning machine." Enterprise Information Systems 17 (2023): 1913764. 10.1080/17517575.2021.1913764. https://doi.org/10.1080/17517575.2021.1913764.

25. Bacanin, N., C. Stoean, M. Zivkovic, D. Jovanovic, M. Antonijevic and D. Mladenovic. "Multi-swarm algorithm for extreme learning machine optimization." Sensors 22 (2022): 4204. https://www.mdpi.com/1424-8220/22/11/4204.

26. Bacanin, N., C. Stoean, D. Markovic, M. Zivkovic, T. A. Rashid, A. Chhabra and M. Sarac. "Improving performance of extreme learning machine for classification challenges by modified firefly algorithm and validation on medical benchmark datasets." Multimedia Tools and Applications (2024): 10.1007/s11042-024-18295-9.

https://doi.org/10.1007/s11042-024-18295-9.

27. Jovanovic, L., M. Gajevic, M. Dobrojevic, N. Budimirovic, N. Bacanin and M. Zivkovic. "Tackling iot security challenge by metaheuristics tuned extreme learning machine." Presented at Intelligent Sustainable Systems, Singapore, 2023. Springer Nature Singapore, 507-22.

28. Saputra, D. C. E., K. Sunat and T. Ratnaningsih. "A new artificial intelligence approach using extreme learning machine as the potentially effective model to predict and analyze the diagnosis of anemia." Healthcare 11 (2023): 697. https://www.mdpi.com/2227-9032/11/5/697.

29. Singh, M. and S. Chauhan. "A hybrid-extreme learning machine based ensemble method for online dynamic security assessment of power systems." Electric Power Systems Research 214 (2023): 108923. https://doi.org/10.1016/j.epsr.2022.108923. https://www.sciencedirect.com/science/article/pii/S0378779622009749.

30. Dai, W., B. Liu, X. Meng and D. Huang. "Spatio-temporal modelling of dam deformation using independent component analysis." Survey Review 46 (2014): 437-43. 10.1179/1752270614y.0000000112. <Go to ISI>://WOS:000346159900009.

31. Dai, W. J., N. Liu, R. Santerre and J. B. Pan. "Dam deformation monitoring data analysis using space-time kalman filter." ISPRS International Journal of Geo-Information 5 (2016): 15. 10.3390/ijgi5120236. <Go to ISI>://WOS:000392493200018.

32. Yang, Z. J., W. J. Dai, R. Santerre, C. L. Kuang and Q. Shi. "A spatiotemporal deformation modelling method based on geographically and temporally weighted regression." Mathematical Problems in Engineering 2019 (2019): 11. 10.1155/2019/4352396. <Go to ISI>://WOS:000506411100003.

33. Chen, S. Y., C. S. Gu, C. N. Lin and M. A. Hariri-Ardebili. "Prediction of arch dam deformation via correlated multi-target stacking." Applied Mathematical Modelling 91 (2021): 1175-93. 10.1016/j.apm.2020.10.028. <Go to ISI>://WOS:000605986800004.

34. Wang, S. W., Y. L. Xu, C. S. Gu, Q. Xia and K. Hu. "Two spatial association-considered mathematical models for diagnosing the long-term balanced relationship and short-term fluctuation of the deformation behaviour of high concrete arch dams." Structural Health Monitoring-an International Journal 19 (2020): 1421-39. 10.1177/1475921719884861. <Go to ISI>://WOS:000496691900001.

35. Cao, W., Z. Wen and H. Su. "Spatiotemporal clustering analysis and zonal prediction model for deformation behavior of super-high arch dams." Expert Systems with Applications 216 (2023): 119439.

36. Léger, P. and M. Leclerc. "Hydrostatic, temperature, time-displacement model for concrete dams." Journal of Engineering Mechanics 133 (2007):

37. Mata, J., A. T. D. Castro and J. S. D. Costa. "Constructing statistical models for arch dam deformation." Structural Control & Health Monitoring 21 (2014): 423-37.

38. Choudhury, T. A., N. Hosseinzadeh and C. C. Berndt. "Improving the generalization ability of an artificial neural network in predicting in-flight particle characteristics of an atmospheric plasma spray process." Journal of Thermal Spray Technology 21 (2012): 935-49. 10.1007/s11666-012-9775-9. <Go to ISI>://WOS:000307521400020.

FUNDING

This work is supported by the Hunan Province Natural Science Foundation, China (Grant No. 2020JJ5571), the Scientific Research Foundation of Hunan Education Department (Grant No. 22B0346) and the Research Foundation of the Department of Natural Resources of Hunan Province (Grant No. HBZ20240115).

ABOUT THE AUTHOR

Jinjin Chen was born in Hunan. China, in 1989. She obtained a master's degree from Central South University in China. She is currently working at Hunan institute of metrology and test. Her main research direction is medical image processing and machine learning methods application.

E-mail: chenjinjin@hnjly.cn

Quan Zhou was born in Hunan. China, in 1992. He obtained a bachelor's degree from University of Shanghai for Science and Technology in China. He is currently working at Hunan institute of metrology and test. His main research direction is machine learning methods application.

E-mail: zhouquan@hnjly.cn

Yueming Cai was born in Hunan. China, in 1995. She obtained a Master's degree from Hunan Agricultural University. She is currently working at Hunan institute of metrology and test. Her main research direction is machine learning methods application.

E-mail:caiyueming@hnly.cn

Bin Liu was born in Hebei, China, in 1988. He obtained a Ph.D. degree from Central South University in China. He currently working at the School of Traffic and Transportation Engineering at Changsha University of Science and Technology in China. His research focuses on the deformation data analysis and modeling.

E-mail: csust_bin@163.com